# Expression of $Na^+$-d-glucose cotransporter SGLT2 in rodents is kidney-specific and exhibits sex and species differences

**Ivan Sabolic, Ivana Vrhovac, Daniela Balen Eror, Maria Gerasimova, Michael Rose, Davorka Breljak, Marija Ljubojevic, Hrvoje Brzica, Anne Sebastiani, Serge C. Thal, Christoph Sauvant, Helmut Kipp, Volker Vallon and Hermann Koepsell**

*Am J Physiol Cell Physiol* 302:C1174-C1188, 2012. First published 18 January 2012;
doi:10.1152/ajpcell.00450.2011

*Am J Physiol Cell Physiol* 302: C1174–C1188, 2012.
First published January 18, 2012; doi:10.1152/ajpcell.00450.2011.

# Expression of $Na^+$-D-glucose cotransporter SGLT2 in rodents is kidney-specific and exhibits sex and species differences

**Ivan Sabolić,[1]* Ivana Vrhovac,[1] Daniela Balen Eror,[1] Maria Gerasimova,[2] Michael Rose,[2] Davorka Breljak,[1] Marija Ljubojević,[1] Hrvoje Brzica,[1] Anne Sebastiani,[3] Serge C. Thal,[3] Christoph Sauvant,[4] Helmut Kipp,[5] Volker Vallon,[2]* and Hermann Koepsell[5]***

[1]*Molecular Toxicology, Institute for Medical Research and Occupational Health, Zagreb, Croatia;* [2]*Medicine and Pharmacology, University of California San Diego and Department of Veterans Affairs San Diego Healthcare System, San Diego, California; and* [3]*Anesthesiology, University of Mainz, Mainz; and* [4]*Physiology and* [5]*Anatomy and Cell Biology, University of Würzburg, Würzburg, Germany*

Submitted 20 December 2011; accepted in final form 13 January 2012

**Sabolić I, Vrhovac I, Balen Eror D, Gerasimova M, Rose M, Breljak D, Ljubojević M, Brzica H, Sebastiani A, Thal SC, Sauvant C, Kipp H, Vallon V, Koepsell H.** Expression of $Na^+$-D-glucose cotransporter SGLT2 in rodents is kidney-specific and exhibits sex and species differences. *Am J Physiol Cell Physiol* 302: C1174–C1188, 2012. First published January 18, 2012; doi:10.1152/ajpcell.00450.2011.—With a novel antibody against the rat $Na^+$-D-glucose cotransporter SGLT2 (rSGLT2-Ab), which does not cross-react with rSGLT1 or rSGLT3, the ~75-kDa rSGLT2 protein was localized to the brush-border membrane (BBM) of the renal proximal tubule S1 and S2 segments (S1 > S2) with female-dominant expression in adult rats, whereas *rSglt2* mRNA expression was similar in both sexes. Castration of adult males increased the abundance of rSGLT2 protein; this increase was further enhanced by estradiol and prevented by testosterone treatment. In the renal BBM vesicles, the rSGLT1-independent uptake of [$^{14}$C]-α-methyl-D-glucopyranoside was similar in females and males, suggesting functional contribution of another $Na^+$-D-glucose cotransporter to glucose reabsorption. Since immunoreactivity of rSGLT2-Ab could not be detected with certainty in rat extrarenal organs, the SGLT2 protein was immunocharacterized with the same antibody in wild-type (WT) mice, with SGLT2-deficient (*Sglt2* knockout) mice as negative control. In WT mice, renal localization of mSGLT2 protein was similar to that in rats, whereas in extrarenal organs neither mSGLT2 protein nor *mSglt2* mRNA expression was detected. At variance to the findings in rats, the abundance of mSGLT2 protein in the mouse kidneys was male dominant, whereas the expression of *mSglt2* mRNA was female dominant. Our results indicate that in rodents the expression of SGLT2 is kidney-specific and point to distinct sex and species differences in SGLT2 protein expression that cannot be explained by differences in mRNA.

immunocytochemistry; mRNA expression; $Na^+$-D-glucose cotransport; proximal tubules

REABSORPTION OF D-GLUCOSE in the renal proximal tubule is of pivotal physiological importance in health and disease. The reabsorption of D-glucose from ultrafiltrate prevents loss of metabolic energy and is important for D-glucose homeostasis and sodium and water balance. In diabetes mellitus, inhibition of D-glucose reabsorption in the proximal tubule may be employed to reduce blood glucose levels (4, 24) and lower glomerular hyperfiltration (47). Bulk reabsorption of ultrafiltrated D-glucose occurs in early proximal tubule via high-capacity/low-affinity $Na^+$-D-glucose cotransport across the brush-border membrane (BBM) and facilitated diffusion of D-glucose across the basolateral membrane (BLM). D-Glucose remaining in the late proximal tubule fluid is reabsorbed by low-capacity/high-affinity $Na^+$-D-glucose cotransport across the BBM and facilitated diffusion across the BLM (6, 45).

After the high-affinity $Na^+$-D-glucose cotransporter SGLT1 (*SLC5A1*) was cloned and the first functional characterization and localization studies were performed, it became clear that SGLT1 is identical with the high-affinity/low-capacity system (21, 52, 53). SGLT1 transports both D-glucose and D-galactose and is mainly expressed in the BBM of small intestine, where it is essential for glucose absorption (16). Patients with defect mutations of *Sglt1* and SGLT1-deficient [*Sglt1*$^{-/-}$, knockout (KO)] mice suffer from the glucose-galactose malabsorption syndrome (16, 33, 52). In the rat kidney, SGLT1 protein is predominantly located in the BBM of proximal tubule S3 segment, showing higher expression and functional activity in females compared with males (5, 38). *Sglt1* KO mice lose ~3% of the filtered glucose in the urine (16). In humans, defect mutations in *Sglt1* did not lead to an obvious renal phenotype, consistent with a minor functional importance of SGLT1 in the kidney under physiological conditions (44).

SGLT subtype SGLT2 (*SLC5A2*) is a low-affinity $Na^+$-D-glucose cotransporter that does not accept D-galactose as substrate. Whereas glucose transport has been shown for various SGLT2 orthologs, SGLT3 from different species has different functional properties. Porcine SGLT3 and mouse (m)SGLT3b are low-affinity $Na^+$-D-glucose cotransporters (2, 31), whereas human SGLT3 proved to be a D-glucose-sensing $Na^+$ channel rather than a transporter (14). Since *Sglt2* mRNA has been demonstrated in renal proximal tubules, and SGLT2 protein has been shown to associate with BBM, SGLT2 is often assumed to be identical with the high-capacity/low affinity $Na^+$-D-glucose transport system in the mammalian kidney (4, 53). In humans, the importance of SGLT2 for renal D-glucose absorption is indicated by renal glycosuria observed in patients with defect mutations of *Sglt2* (39). A recent study by Vallon et al. (48) using *Sglt2*-deficient mice as negative control demonstrated that SGLT2 protein is expressed and mediates glucose reabsorption in the early proximal tubule and most of the glucose reabsorption by the kidney overall. The remaining fraction of glucose may be reabsorbed by SGLT1 or by the $Na^+$-D-monosaccharide cotransporter NaGLT1 (22). NaGLT1, a low-affinity $Na^+$-D-glucose cotransporter that does not trans-

* I. Sabolić, V. Vallon, and H. Koepsell contributed equally to the experimental design and manuscript writing.

Address for reprint requests and other correspondence: I. Sabolić, Unit of Molecular Toxicology, Institute for Medical Research and Occupational Health, Ksaverska cesta 2, HR-10001 Zagreb, Croatia (e-mail: sabolic@imi.hr).

port D-galactose, has been cloned from rat and is highly expressed in kidney, where it is located in the BBM of proximal tubules (22).

SGLT2 has been cloned from human (25, 51), pig (26, 31), rat (54), mouse (41), and bovine (57). The distribution of SGLT2 was mainly investigated on the mRNA level by Northern blot analysis and in situ hybridization. In rat, high concentrations of *Sglt2* mRNA were found in the renal proximal tubule S1 segments and less in the S2 segments, whereas the S3 segments were negative (54). In bovine, low concentrations of *Sglt2* mRNA were also observed in small intestine, liver, lung, spleen, mammary gland, skeletal muscle, and ciliary epithelium (12, 56, 57). In humans, by real-time PCR the highest concentration of *Sglt2* mRNA was observed in kidneys, but a limited expression was also detected in various extrarenal organs/tissues including small intestine, liver, brain, prostate, and testis (59), whereas recent studies indicated a highly kidney-specific expression of *Sglt2* mRNA (13). Western blots and immunocytochemical studies using commercial polyclonal antibodies against SGLT2 have been reported. Whereas the antibodies allowed labeling of SGLT2-related bands in Western blots (7, 18, 35, 42), the immunocytochemical studies did not reveal staining that allowed visualization of details (7).

To elucidate SGLT2 functions in health and disease, a detailed knowledge concerning expression of the transporter in kidney and other organs is required. This includes sex differences and changes of intracellular distribution during posttranscriptional regulations as has been described for SGLT1 (5, 27, 35, 38, 49). Localization of SGLT2 protein in rodents and humans is also required to anticipate potential side effects of selective SGLT2 inhibitors that are being developed by pharmaceutical companies for treating diabetic hyperglycemia (4, 20, 23). To determine sites of expression and locations of SGLT2 in male and female rats (rSGLT2), we generated a novel polyclonal antibody against the rat protein that allows detection of SGLT2 in Western blots and by immunocytochemistry. The antibody cross-reacts with mSGLT2 and has been recently applied to demonstrate an absence of mSGLT2 protein in the nephron of *Sglt2* KO mice (48). Here we used this antibody, aiming to *1*) characterize it as a novel, specific tool to study the SGLT2 protein expression in rat and mouse organs and *2*) address the differences in SGLT2 expression in male versus female rats and mice. The major findings at the protein level were correlated with the expression of *Sglt2* mRNA.

## MATERIALS AND METHODS

### *Animals and Treatment*

Adult (10–12 wk old) and prepubertal (25 days old) male and female and young (6 wk old) male Wistar strain rats were from the breeding colony at the Institute in Zagreb. Adult male and female C57BL/6 mice (3–4 mo old), used for testing sex and species differences in mSGLT2 protein expression, were obtained from the breeding colony at the Institute Rudjer Bošković in Zagreb. Animal care and treatment were conducted in conformity with institutional guidances that are in compliance with international laws. Before and during experiments, animals had standard pelleted food and tap water ad libitum. The studies were approved by the Institutional Ethics Committee.

Kidneys of intact adult (age 3–4 mo) male and female rats and mice were used to study sex and species differences. To study effects of castration and ovariectomy in adult rats, males were castrated by the scrotal route and females were ovariectomized by a dorsal approach under Narketan-Xylapan anesthesia. The sham-operated animals underwent the same procedure, but their respective organs were not removed. The operated animals were left to recover for 4 wk before death. Prepubertal rats were used intact. To study effects of hormonal treatment in rats, young males were either sham operated or castrated and left to recover for another 6 wk. The castrated rats then underwent subcutaneous treatment with testosterone enanthate, estradiol dipropionate, or progesterone at a dose of (each) 2.5 mg·kg body mass$^{-1}$·day$^{-1}$ for 14 days (every day except Sunday). The hormones were injected as a sunflower oil solution. The castrated control and sham-operated rats were treated subcutaneously with equivalent amounts of sunflower oil (0.5 ml·kg body mass$^{-1}$·day$^{-1}$ for 14 days). As recently reported, such operations and treatments in rats caused a distinct expression pattern of the basolateral (OAT1, OAT3) and brush border (OAT2, OAT5) organic anion transporters (OATs) and SGLT1 in proximal tubules (5, 11, 29, 30, 38). The studies in mice were performed in tissue samples taken from intact adult (3–4 mo old) male and female animals.

### *SGLT2-Deficient Mice*

SGLT2-deficient (*Sglt2* KO; *Sglt2*$^{-/-}$) mice and relevant control mice [wild type (WT); *Sglt2*$^{+/+}$ mice] were obtained from two sources. One source was previously described in detail by Vallon et al. (48) and was used to test protein and mRNA expression in the kidneys and other organs. Another (commercial) source was the Wellcome Trust Sanger Institute Mouse Genetics Project [KOMP-CSD Project: 36435; strain C57BL/6J-Tyr; C57BL/6N-Slc5a2$^{tm1a(KOMP)Wtsi}$]. Details of the allele and targeting strategy can be found at **http://www.knockoutmouse.org/martsearch/project/36435**. These animals were used for immunochemical studies in kidneys and other organs and for mRNA studies in kidneys.

### *Antibodies and Other Material*

Polyclonal immune serum against the 18-meric peptide specific for rSGLT2 (amino acids 592–609: AMGIEEVQSPAPGLLRQC) was raised in rabbits. A BLAST search of the GenBank database indicated that the amino acid sequence in this peptide is 61%, 67%, 83%, 61%, and 78% homologous to the corresponding peptide in human, bull, mouse, dog, and rabbit SGLT2, respectively. It showed no homology to rSGLT1, pig SGLT2, rNaGLT1, and mSGLT4. The BLAST search also indicated no other proteins in the rat and mouse tissues containing a significant part of this peptide sequence. The antibody (rSGLT2-Ab) was affinity purified from the immune serum via antigenic peptide-coupled support (15). Monoclonal antibodies against α-actin (actin-Ab) and β-actin (β-actin-Ab) were purchased commercially from Chemicon International (Temecula, CA) and Sigma-Aldrich (St. Louis, MO), respectively. The use of rabbit-raised polyclonal antibody against the cell adhesion molecule CAM105 (CAM105-Ab) in immunochemical studies has been described previously (37).

Secondary antibodies labeled with fluorescent markers or alkaline phosphatase were purchased commercially from Jackson ImmunoResearch Laboratories (West Grove, PA) or Kirkegaard and Perry (Gaithersburg, MD), and included Cy3-labeled (GARCY3), FITC-labeled (GARF), or alkaline phosphatase-labeled (GARAP) goat anti-rabbit IgG and alkaline phosphatase-labeled goat anti-mouse IgG (GAMAP). The fluorescence fading retardant Vectashield was purchased from Vector Laboratories (Burlingame, CA).

Oil solutions of testosterone enanthate, estradiol dipropionate, and progesterone were from RotexMedica (Trittau, Germany) and/or Galenika (Belgrade, Serbia). The molecular weight standards used in immunoblotting were from Bio-Rad (Hercules, CA). [$^{14}$C]-α-methyl-D-glucopyranoside ([$^{14}$C]AMG; 11.7 GBq/mmol) was purchased from Amersham Biosciences (Freiburg, Germany). Complete Protease Inhibitor cocktail was from Roche (Indianapolis, IN). All other chem-

icals and reagents were analytical or MB grade, obtained from commercial sources such as Sigma-Aldrich or Fisher Scientific. Specific provisions for immunochemical experiments in tissues of WT and *mSglt2* KO mice are indicated in the text related to these studies (vide infra).

*Tissue Fixation and Immunocytochemistry*

Detailed steps in fixation of rat organs in vivo, preparation of tissue cryosections, and immunofluorescence cytochemistry were described in our recent study on rSGLT1 (38). Briefly, in anesthetized adult rats the circulatory system was perfused via the left ventricle of the heart, first with phosphate-buffered saline (PBS, in mM: 137 NaCl, 2.7 KCl, 8 $Na_2HPO_4$, 2 $K_2PO_4$, pH 7.4) to remove blood and then with fixative (4% *p*-formaldehyde in PBS). Various organs (cerebrum, cerebellum, eyes, submaxillary gland, heart, lungs, spleen, pancreas, liver, small intestine, abdominal fat tissue, testes, uterus, skeletal muscle) were removed, sliced, kept in the same fixative overnight, then extensively washed in PBS, and stored in PBS containing 0.02% $NaN_3$ at 4°C. When needed, 4-μm-thick cryosections of the fixed tissue were cut and collected on Superfrost/Plus microscope slides, dried at room temperature, and kept refrigerated until use.

Prepubertal rats and mice were killed by cervical dislocation, the abdominal cavity was opened, and large abdominal blood vessels were cut and bled out under a stream of running water. The kidneys and other organs were removed, rinsed with cold PBS, sliced, immersion fixed overnight, and further processed as described for organs from the adult rats (vide supra).

Before application of the primary antibody, cryosections underwent an antigen retrieval procedure, as described in detail previously for SGLT1 in the rat kidneys (5). In preliminary experiments we confirmed that the same antigen retrieval is optimal for tissue cryosections of both rat and mouse organs (data not shown). In short, the dried cryosections underwent rehydration in PBS, heating in 10 mM citrate buffer, pH 6, in a microwave oven, cooling down to room temperature in the same buffer, incubation in 0.5% Triton X-100, and rinsing with PBS. The steps were incubation in bovine serum albumin (1% in PBS) to block nonspecific antibody binding, incubation with rSGLT2-Ab (1:5,000–1:100 in PBS) overnight at 4°C, rinsing with PBS, incubation in GARCY3 (1:800; 1.6 μg/ml PBS) at room temperature for 60 min, rinsing with PBS, cover with Vectashield, and inspection for fluorescence.

To localize the rSGLT2-related immunostaining in specific nephron segments of the rat kidney, consecutive cryosections were stained for rSGLT2 and CAM105. Our previous study in rats showed strong staining of CAM105 in the brush border of S1 and S3 proximal tubule segments, weak to negative staining of brush border in the S2 segment, and limited staining of the glomerular and peritubular capillaries (37). After antigen retrieval at pH 6, consecutive sections were stained either with rSGLT2-Ab (1:200) or CAM105-Ab (1:200 in PBS) overnight at 4°C, rinsed with PBS, incubated with secondary antibodies [GARCY3 (1.6 μg/ml PBS) or GARF (15 μg/ml PBS), respectively] for 1 h at room temperature, rinsed with PBS, covered with Vectashield, and inspected for fluorescence.

To test the specificity of rSGLT2-Ab for the immunizing peptide, the antibody was blocked with the peptide (final concentration: 0.5 mg/ml) for 4 h at room temperature prior to use in the above-described immunocytochemical assay.

The stained sections were examined and photographed with an Opton III RS fluorescence microscope (Opton Feintechnik, Oberkochen, Germany) using a Spot RT Slider camera and software (Diagnostic Instruments, Sterling Heights, MI). All images to be used for comparative purposes were recorded with the same software parameters. The images were imported into Adobe Photoshop 6.0 for processing and labeling. In images taken after a single staining, the red fluorescence of Cy3 was converted into black-and-white mode with the same software.

*Preparation and Western Blotting of Tissue Homogenates and Cell Membranes for Studying Sex and Species Differences of SGLT2 in Rat and Mouse Kidneys*

Animals were killed by decapitation. Kidneys were removed, decapsulated, and either used in toto (prepubertal rats and adult mice) or sagittally sectioned in ~2-mm-thick slices (intact, gonadectomized, and hormone-treated adult rats). From these slices, the cortex and outer stripe were dissected manually and used as separate tissue pools. The whole small intestine was removed, opened longitudinally, and rinsed with cold PBS, and the mucosa was scraped and further processed.

The details of tissue homogenization and differential centrifugation of the homogenates in refrigerated centrifuges were described previously (38). Total cell membranes (TCM) were collected as the 150,000 g pellet from a 6,000 g supernatant. BBM from the rat kidneys (whole kidneys, kidney cortex, outer stripe) and small intestinal mucosa, as well as from the whole kidneys of prepubertal rats and adult mice, were isolated by the $MgCl_2$ precipitation method (9). The final membrane preparations were resuspended in buffer (in mM: 150 mannitol, 2.5 EGTA, 12 Tris·HCl, pH 7.4), and stored at −70°C until use in immunoblotting studies. Protein was measured by the Bradford assay (10).

As tested in preliminary experiments (data not shown), the same conditions for SDS-PAGE and Western blotting are valid with both rat and mouse membranes. Denaturation of membrane samples in Laemmli buffer [±β-mercaptoethanol (β-ME)] and heating at different temperatures (37°C for 30 min, 65°C for 15 min, 95°C for 5 min), separation of the proteins through 10% SDS-PAGE minigels, as well as electrophoretic wet transfer to an Immobilon membrane (Millipore, Bedford, MA) were performed as described previously (5, 38). The amount of protein per well is indicated in figures. The transfer membrane was blocked in 5% milk protein-containing blotting buffer (38), incubated at 4°C overnight in the same buffer containing rSGLT2-Ab (1:1,000) or actin-Ab (0.5 μg/ml), washed in blotting buffer, and incubated for 60 min in the same buffer that contained GARAP (0.1 μg/ml) or GAMAP (0.1 μg/ml), respectively. Then the membrane was washed and stained for alkaline phosphatase activity with the 5-bromo-4-chloro-3-indolyl phosphate (BCIP)/nitro blue tetrazolium (NBT) assay as an indicator (5, 38). Labeled protein bands were evaluated by densitometry with Quantity One 1-D Analysis Software (Bio-Rad Laboratories); an area of the broadest 75-kDa protein band of rSGLT2 in the blot was marked, and an equal area was applied to all other bands in the same blot. The same approach was applied for evaluating the 42-kDa protein band of α-actin. The area density of each band was expressed in arbitrary densitometric units, relative to the strongest band density (= 100 relative densitometric units) in the corresponding control samples.

To demonstrate the specificity of rSGLT2-Ab for the immunizing peptide, rSGLT2-Ab was preincubated with the peptide (final concentration: 0.5 mg/ml) for 4 h at room temperature and then used in an immunoblotting assay as described above.

*Extrarenal Expression of SGLT2 Protein in WT and KO Mice*

WT and *Sglt2* KO mice (48) were anesthetized with ketamine-xylazine, and various organs were rapidly harvested and immediately frozen in liquid nitrogen for later analyses. For mSGLT2 protein analysis, organs were thawed and homogenized in a buffer containing 250 mM sucrose, 10 mM triethanolamine, and protease inhibitors with a tissue homogenizer (Tissumizer; Tekmar, Cincinnati, OH). Protein concentration was determined with a DC Protein Assay (Bio-Rad).

The protein samples were diluted in 4× LDS sample buffer (Invitrogen, Carlsbad, CA), heated for 15 min at 65°C, and loaded on precast 4–12% Bis-Tris SDS-PAGE gels (Invitrogen) with MOPS buffer. After electrophoretic transfer to nitrocellulose membrane, the membrane was blocked with 5% nonfat dry milk in PBS (pH 7.4) containing 0.1% Tween 20 for 1 h. Immunoblotting was performed at

4°C overnight with the rSGLT2-Ab diluted 1:1,000 as described previously (48). Chemiluminescent detection was performed with a 1:5,000 dilution of ECL donkey anti-rabbit IgG linked to horseradish peroxidase and ECL detection reagent purchased from GE Healthcare (Chalfont St Giles, UK). To verify equal protein loading between genotypes, the membrane was stripped with 0.2 M NaOH for 5 min and reprobed with monoclonal β-actin-Ab.

*Transport Assay in Rat Renal Brush-Border Membrane Vesicles*

BBM vesicles were isolated by the $MgCl_2$ precipitation method (9) from whole kidney homogenates of adult male and female rats. The vesicles were resuspended in buffer (100 mM mannitol, 20 mM HEPES-Tris, pH 7.1), snap-frozen in liquid nitrogen, and stored at −70°C until further use for transport measurements.

The uptake of [$^{14}$C]AMG into BBM vesicles at 22°C was initiated by adding 20 μl of the thawed and temperature-equilibrated BBM vesicle suspension to 50 μl of incubation medium. The final composition of the incubation medium was (in mM) 100 mannitol, 100 NaSCN, 20 mM HEPES-Tris, pH 7.4, and 0.1 [$^{14}$C]AMG. SGLT1-related transport was inhibited by adding 20 mM galactose. The remaining transport activity was inhibited by addition of 0.2 mM phlorizin. The reaction was terminated after 5 s by dilution with 1 ml of ice-cold stop solution (in mM: 100 mannitol, 100 NaCl, 0.2 phlorizin, and 20 HEPES-Tris, pH 7.4). Extravesicular radioactivity was removed by filtration on nitrocellulose filters, which were rinsed with 3.5 ml of ice-cold stop solution. The filters were treated with scintillation fluid, and the radioactivity was counted in a liquid scintillation counter.

*Real-Time RT-PCR in Rat Kidneys*

RNA from the whole kidney of male and female rats was extracted with the Qiagen RNeasy Mini Kit. RNA concentration was determined, and cDNA was synthesized with the iScript cDNA synthesis kit (Bio-Rad) according to the manufacturer's instructions. In brief, real-time RT-PCR was performed according to the iQ SYBR Green Supermix RT-PCR system protocol (Bio-Rad). Initial denaturation was performed at 95°C for 3 min. The PCR amplification cycle was performed as follows: denaturation step at 95°C for 15 s, annealing step at 65°C for 30 s, and elongation step at 72°C for 30 s. The latter cycle was repeated 45 times. Primers for the *rSglt2* (*rSlc5a2*) mRNA (NCBI accession no. NM_022590.2) were chosen as published by Takahashi et al. (43); the primers were 5′-CATTGTCTCAGGCTGGCACTGG-3′ (sense) and 5′-GGTGTTCATTGTGGCAGTGTCC-3′ (antisense), resulting in a 460-bp RT-PCR product. Quantification was performed by the $\Delta\Delta C_t$ method (where $C_t$ is threshold cycle) with β-actin as a reference, and the expression in males was taken as a control (normalized to 100). For β-actin, the primers were 5′-TCTACAATGAGCTGCGTGTG-3′ (sense) and 5′-TACATGGCTGGGGTGTTGAA-3′ (antisense), resulting in a 129-bp RT-PCR product. Primers were chosen to span introns in order to avoid false positive results due to contamination with genomic DNA. The RT-PCR products were tested for correct size by melting point analysis and agarose gel electrophoresis. Subsequently, the respective PCR products were excised, extracted, and analyzed in a 3130 Genetic Analyzer (Applied Biosystems) (data not shown).

*Real-Time RT-PCR in Mouse Organs*

For *mSglt2* mRNA analysis in various organs of WT and *Sglt2* KO mice (48), tissues were homogenized in Buffer RLT from an RNeasy Mini Kit (Qiagen, Valencia, CA) with a rotor-stator homogenizer (Tissumizer; Tekmar). Tissue RNA was prepared with an RNeasy Mini Kit and was quantified by Nanodrop. cDNA was prepared with the SuperScript II First Strand Synthesis System (Invitrogen). For quantification of *mSglt2*, a TaqMan gene expression assay (Mm00453831_m1) was performed with TaqMan Universal PCR Master Mix in an ABI 7300 Real Time PCR System as described previously (48). Amplification efficiencies were normalized against the housekeeping gene *rpl19* (forward: 5′-TGCTCAGGCTACAGAAGAGGCTTG-3′, reverse: 5′-GGAGTTGGCATTGGCGATTTC-3′), and relative fold increases were calculated. All PCR reactions were performed with 1 μg of cDNA (RNA equivalent) under the following conditions: 10 min at 95°C with 50 cycles of 15 s at 95°C and 1 min at 60°C. Each experiment was performed in triplicate.

*Statistical Analysis*

The numeric data, expressed as means ± SE, were statistically evaluated by Student *t*-test or ANOVA with post hoc Duncan test at the 5% level of significance.

## RESULTS

### *SGLT2 in Rat Organs*

*Specificity of rSGLT2-Ab.* The specificity of rSGLT2-Ab was tested by immunoblotting of TCM and BBM prepared from the female kidney cortex and by immunostaining of cryosections from kidney and small intestine. As shown in Fig. 1*A*, in both reducing (+β-ME) and nonreducing (−β-ME) conditions the antibody consistently labeled a broad protein band with an apparent molecular mass of ~75 kDa. Density of the band was temperature dependent and stronger in nonreducing conditions. The strongest reactions were obtained after denaturation under nonreducing conditions at 37°C for 30 min or at 65°C for 15 min. In all further experiments, isolated membranes were denatured in nonreducing conditions at 65°C for 15 min. In TCM (Fig. 1*B*) and BBM (Fig. 1*C*) isolated from the female kidney cortex, strong labeling of the ~75-kDa band was observed. The band was absent in TCM isolated from the small intestinal mucosa of the same animal (Fig. 1*B*) and in the renal TCM and BBM after block of rSGLT2-Ab with the antigenic peptide (Fig. 1, *B* and *C*, Ab+P).

In cryosections of the female kidney cortex, with optimal experimental conditions for antigen retrieval and staining, rSGLT2-Ab strongly stained the brush border of S1 and S2 segments of proximal tubules (Fig. 1 *D*, K). In contrast, rSGLT2-Ab did not stain the brush border of small intestine of the same animal (Fig. 1*D*, I), which strongly reacted with an antibody against rSGLT1 (5). rSGLT2-Ab immunoreactivity in kidney cortex was abolished when rSGLT2-Ab had been absorbed with the antigenic peptide (Fig. 1*D*, K+P). The intensity of background staining observed in small intestine and kidney treated with the absorbed rSGLT2-Ab was similar to the staining obtained with the secondary antibody alone (data not shown).

*Location of rSGLT2 in renal cortex and outer stripe.* As further shown in female kidneys, staining of the long-villi brush border in S1 segments of renal proximal tubules in superficial and deep cortex (Fig. 1*E*, asterisks) was stronger compared with the short-villi brush border in S2 segments (Fig. 1*E*, arrows). The S3 segments of proximal tubules in medullary rays (not shown) and in the outer stripe (Fig. 1*E*, arrowheads) were not stained. No staining of other nephron segments was observed (not shown). In Western blots of TCM from the female kidney zones, strong rSGLT2-Ab immunoreactivity of the 75-kDa band was observed in the

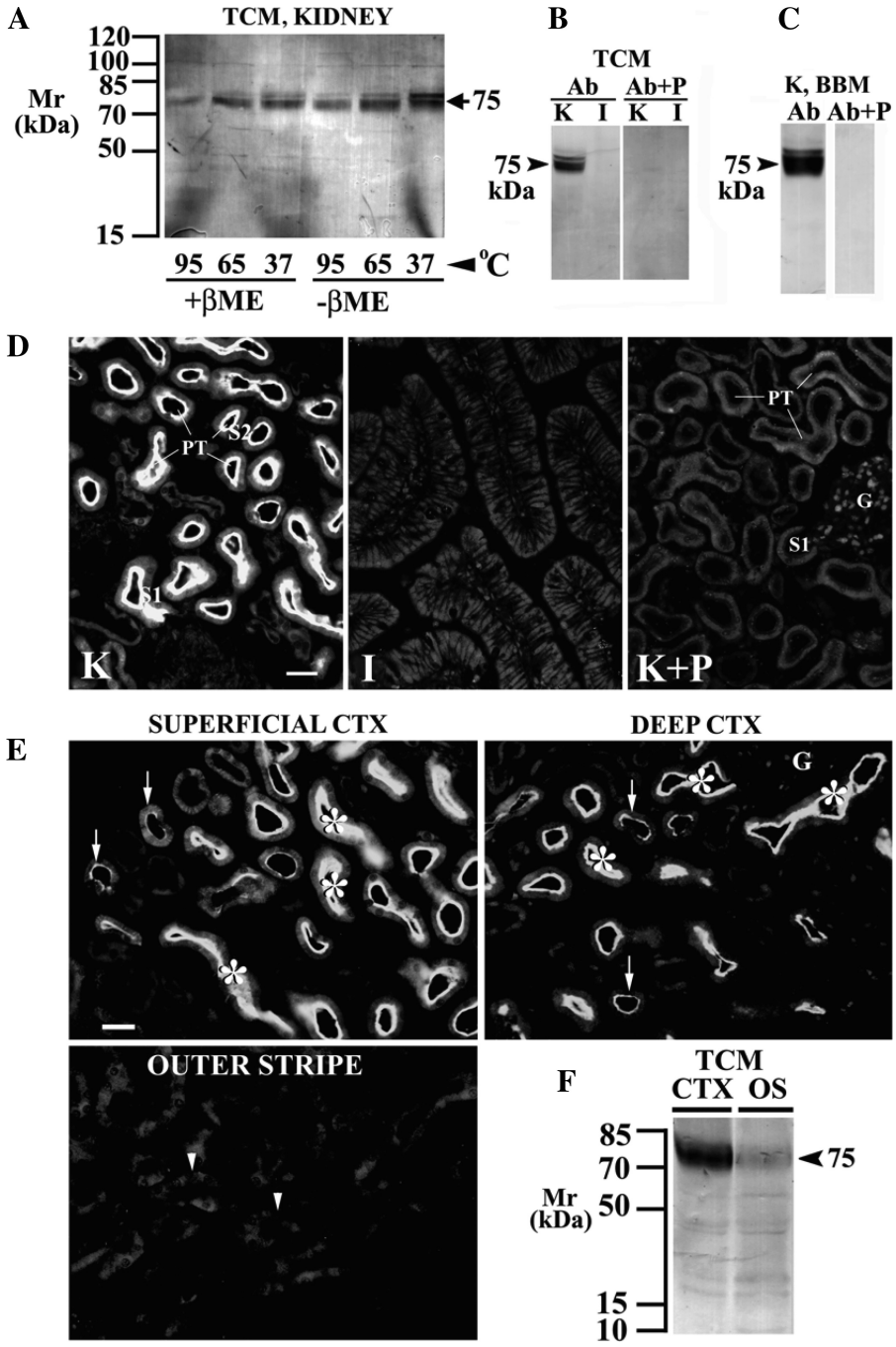


Fig. 1. Immunoreactivity of antibody against rat SGLT2 (rSGLT2-Ab) in kidneys and small intestine of female rats. *A*: optimal conditions for Western blots with total cell membranes (TCM) from rat kidney cortex. For SDS-PAGE, isolated TCM were prepared in Laemmli buffer with (+β-ME) or without (−β-ME) β-mercaptoethanol and heated for 5 min at 95°C, 15 min at 65°C, or 30 min at 37°C. In all conditions, only a broad ~75-kDa protein band was labeled. *B*: Western blot of TCM isolated from the rat kidney cortex (K) or mucosa of the small intestine (jejunum; I) with rSGLT2-Ab (Ab) or with the antigenic peptide-blocked rSGLT2-Ab (Ab+P). Each lane in *A* and *B* contained 60 μg of protein. *C*: Western blot of brush-border membrane (BBM) isolated from whole rat kidneys with the native (Ab) or peptide-blocked (Ab+P) rSGLT2-Ab. Each lane contained 40 μg of protein. Denaturation of the membranes for *B* and *C*, as well as in all further experiments, was performed for 15 min at 65°C (−β-ME). *D*: immunostaining of kidney cortex (K) and small intestine (I) with rSGLT2-Ab or with the peptide-blocked rSGLT2-Ab (K+P). In kidney cortex (K), rSGLT2-Ab strongly stained the brush border of proximal tubules, while the brush border of villi in intestine remained unstained. After preabsorption of rSGLT2-Ab with the antigenic peptide, no staining of renal cortical tubules was observed (K+P). G, glomerulus; PT, proximal tubule; S1, S1 segment; S2, S2 segment. *E*: zonal differences: rSGLT2-Ab immunoreactivity in superficial and deep cortex and in outer stripe. rSGLT2-Ab exclusively stained the BBM of cortical proximal tubules; staining in the S1 segments (asterisks) was stronger compared with the S2 segments (arrows). Data represent findings in 3 female rats. G, glomerulus. S3 segments in the outer stripe (arrowheads) were not stained. Bars in *D* and *E*, 20 μm. *F*: Western blot of TCM isolated from the rat kidney cortex (CTX) or outer stripe (OS). The experiment was performed as in *B*. Prominent staining of the 75-kDa protein band was only observed in cortical membranes.

kidney cortex (Fig. 1*F*, CTX), whereas in the outer stripe only a faint 75-kDa band was detected (Fig. 1*F*, OS). This faint band is probably due to incomplete separation of the outer stripe from the cortex.

The segment-specific localization of rSGLT2 in the rat proximal tubule was confirmed with consecutive sections of the female kidney stained with rSGLT2-Ab (Fig. 2, *A* and *C*) and CAM105-Ab, which reacts strongly with S1 and S3 segments of rat proximal tubules and shows only very weak staining of S2 segments (37) (Fig. 2, *B* and *D*). In the cortex, strong staining of rSGLT2 and CAM105 (arrowheads) was colocalized in the high brush border of S1 segments, whereas the lower brush border of S2 segments exhibited weaker staining of rSGLT2 and no or very weak staining of CAM105 (Fig. 2, *A* and *B*). In the outer stripe, the brush border of S3 segments was negative for rSGLT2 (Fig. 2*C*) and strongly positive for CAM105 (Fig. 2*D*, arrowheads). The observed immunocytochemical distribution of rSGLT2 is consistent with previous in situ hybridization data in the rat kidney (54) and with transport data in isolated membrane vesicles from the rabbit kidney (45), where expression of SGLT2 mRNA and low-affinity glucose transport, respectively, were detected in cortical but not in medullary tubules. Our data thus provide evidence that in rats the rSGLT2 protein is exclusively expressed in the S1 and S2 segments of renal proximal tubules with the intensity pattern S1 > S2.

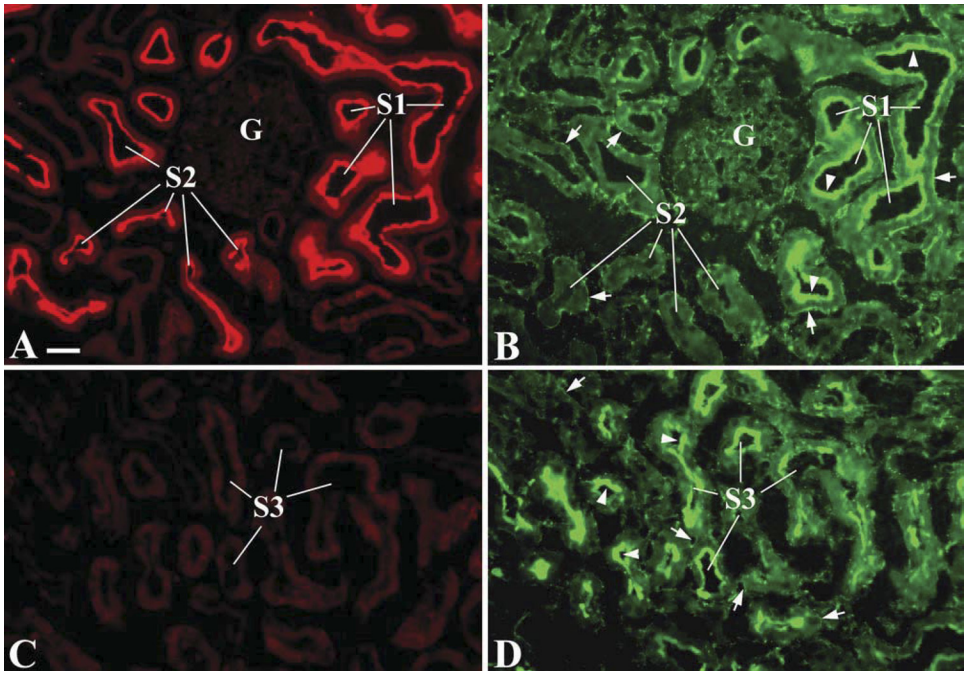


Fig. 2. Immunolocalization of rSGLT2 and cell adhesion molecule CAM105 in proximal tubular segments. Staining with rSGLT2-Ab (*A*, *C*) and CAM105-Ab (*B*, *D*) was performed in consecutive sections of rat kidney cortex (*A*, *B*) and outer stripe (*C*, *D*). In cortex (*A*), rSGLT2-Ab stained the high brush border of S1 segments and the low brush border of S2 segments. In accordance with previous data (37), these segments can be distinguished by BBM staining with CAM105-Ab, which is strong in the S1 segment (*B*, arrowheads) and weak or absent in the S2 segment (*B*). In the outer stripe, the brush border of S3 segments was negative for rSGLT2 (*C*) and strongly positive for CAM105 (*D*, arrowheads). Data represent findings in 2 female rats. Cell membranes of the glomerular (G) and peritubular capillaries (arrows, *B* and *D*) were also positive for CAM105. Bar, 20 μm.

*Sex differences in expression of rSGLT2 in adult but not in prepubertal rats.* Comparison of the rSGLT2-Ab-related immunostaining in male and female kidneys of adult rats revealed the presence of sex differences; the staining intensity of the brush border in cortical proximal tubules in males was weaker than in females (Fig. 3*A*). These sex differences were confirmed by Western blotting of BBM isolated from the kidney cortex; the density of the rSGLT2-related 75-kDa protein band was approximately threefold higher in the membranes from females, whereas the density of the α-actin band was similar in both sexes (Fig. 3, *B* and *C*). However, the quantitative RT-PCR data showed similar amounts of *Sglt2* mRNA in the renal cortex of adult male and female rats (Fig. 3*D*).

Expression of the rSGLT2 protein in kidney cortex was further determined in prepubertal (age: 25 days) rats of both sexes and compared with that in adult males and females (Fig. 3, *E–G*). As shown in Fig. 3*E*, the staining intensity of brush border in the cortical proximal convoluted tubules in prepubertal males (PPM) and females (PPF) were similar and lower than in adult male (AM) or female (AF). This pattern was confirmed by immunoblotting of BBM isolated from the whole kidneys (Fig. 3, *F* and *G*). The density of the 75-kDa band in membranes from prepubertal male and female rats was similar but ~50% and ~75% weaker than in adult males and females, respectively. Overall, these data indicate that sex differences in the renal expression of rSGLT2 in rats are posttranscriptionally upregulated after puberty.

*Effect of gonadectomy and replacement therapy with sex hormones on renal expression of rSGLT2 protein.* To determine the sex hormone(s) responsible for the observed sex differences in renal expression of rSGLT2 protein, *1*) male and female rats were gonadectomized at the age of 6 wk and the renal rSGLT2 protein expression analyzed 6 wk later (Fig. 4, *A–D*) and *2*) castrated males were treated for 2 wk before death with testosterone, estradiol, or progesterone (Fig. 4, *E–G*). As shown in Fig. 4, *A* and *B*, castrated males exhibited an enhanced (~45%) density of the rSGLT2-related 75-kDa protein band in isolated renal cortical BBM compared with sham-operated animals, whereas the α-actin protein band was unchanged. The castration-induced upregulation of rSGLT2 expression was also observed by immunostaining (Fig. 4*E*, compare sham-operated oil-treated rats with castrated oil-treated rats). At variance with castration, ovariectomy in females did not significantly affect the rSGLT2-related protein band in the cortical BBM preparations (Fig. 4, *C* and *D*). Also, no major change of the rSGLT2-related immunostaining of cortical proximal tubules was observed after ovariectomy (data not shown). The castration experiments suggested that androgens inhibit the expression of rSGLT2 protein in rat renal proximal tubules. Since no intracellular staining with rSGLT2-Ab was observed in males and females (Fig. 3*A*), the androgen effect appeared to be due to regulation of the total amount of rSGLT2 protein in the cells rather than to changes in rSGLT2 trafficking. To test this interpretation, castrated males were treated with either oil or various sex hormones dissolved in the same oil and the rSGLT2 protein abundance in TCM from the cortex was quantified (Fig. 4, *E–G*). By immunocytochemistry, the enhanced staining of rSGLT2 in brush border of cortical proximal tubules observed after castration was reversed by testosterone treatment. Treatment with estrogen additionally enhanced the staining of rSGLT2, whereas progesterone treatment slightly diminished the staining intensity (Fig. 4*E*). The Western blot data for TCM from the kidney cortex showed that the enhanced rSGLT-related 75-kDa band density in castrated animals was strongly downregulated by testosterone or progesterone but additionally upregulated by estradiol (Fig. 4, *F* and *G*). In contrast, labeling of the α-actin band was not affected by the hormonal treatments.

*D-Galactose-sensitive and D-galactose-insensitive $Na^+$-D-glucose cotransport in BBM vesicles isolated from adult male and female rats.* In this experiment we tested whether the higher expression of rSGLT2 protein in BBM isolated from the

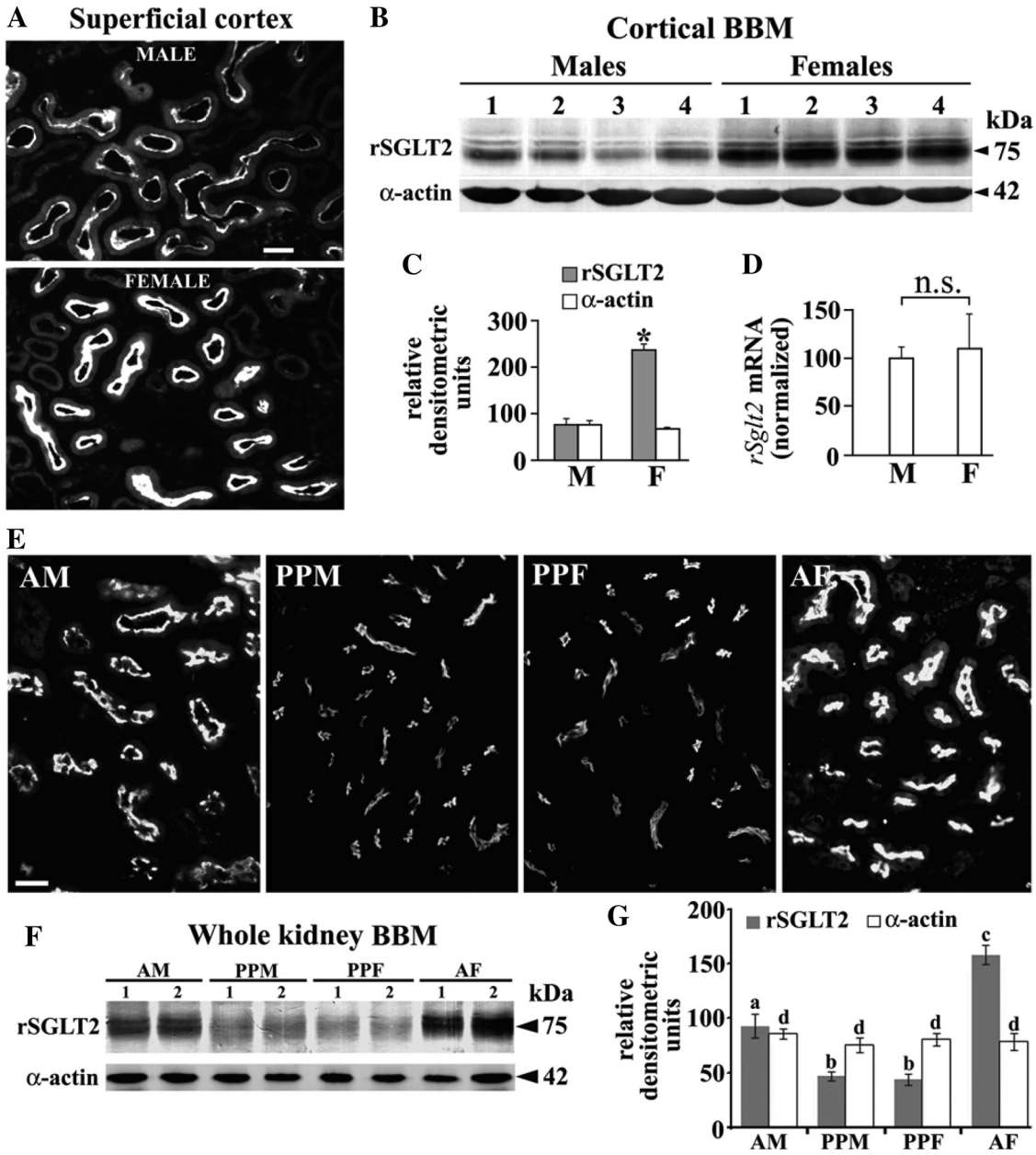


Fig. 3. Sex-dependent expression of rSGLT2 in kidneys of adult (*A–D*) and prepubertal (*E–G*) rats. *A*: immunostaining with rSGLT2-Ab in cortical proximal tubules of an adult male (M) and female (F) rat. The staining intensity of the proximal tubule brush border in the M was weaker than in the F. Data represent findings in 2 animals of each sex. Bar, 20 μm. *B*: abundance of rSGLT2 protein and α-actin in isolated renal cortical BBM from 4 adult M and F. Each lane contained 40 μg protein. *C*: densitometric evaluation of the bands shown in *B*; the rSGLT2-related 75-kDa protein band was ~3-fold stronger in adult F compared with adult M (*$P < 0.05$), whereas the α-actin-related 42-kDa protein band showed no sex differences. *D*: expression of *rSglt2* mRNA in kidneys of adult M and F as estimated by real-time RT-PCR ($N = 5$ for each sex). No significant sex difference was detected (n.s., not significant). *E*: comparison of rSGLT2-Ab immunostaining in the renal cortex of adult M (AM), prepubertal M (PPM) and F (PPF), and adult F (AF) rats. Whereas adult animals exhibited stronger staining in females, the staining in prepubertal rats was much weaker than in the adult rats and sex independent. In control experiments, the staining in both adult and prepubertal rats was abolished when rSGLT2-Ab was preincubated with the antigenic peptide (not shown). Data represent findings in 3 rats of each sex. Bar, 20 μm. *F*: representative immunoblots of rSGLT2 and α-actin in BBM isolated from the whole kidneys of adult (AM and AF) and prepubertal (PPM and PPF) rats. Immunoblots were performed with 60 μg protein/lane. *G*: densitometric quantification of the rSGLT2-related 75-kDa protein band ($N = 4$ for each group). In PPM and PPF the rSGLT2-related bands showed similar intensity; they were ~50% weaker than in adult M and ~70% weaker than in adult F. The α-actin band was age- and sex independent. Statistics (ANOVA/Duncan test): $P < 0.05$: a/b, a/c, and b/c; n.s.: b/b and d/d.

renal cortex of females versus males correlated with the activity of D-galactose-insensitive, phlorizin-inhibitable $Na^+$-D-glucose cotransport (Fig. 5). The sodium gradient-driven uptake of 0.1 mM [$^{14}$C]AMG was tested in isolated BBM vesicles by the rapid filtration technique. AMG is a substrate for $Na^+$-D-glucose cotransporters SGLT1, SGLT2, and NaGLT1 (22, 34, 54) but not for sodium-independent glucose facilitators of the GLUT family (8, 22, 34, 54). At variance with the GLUT transporters, rSGLT1, rSGLT2, and NaGLT1 are inhibited by phlorizin. Since D-galactose is transported by rSGLT1 but not by rSGLT2 or NaGLT1 (22, 34, 54), the AMG uptake inhibited by 20 mM D-galactose represented the rSGLT1-related AMG

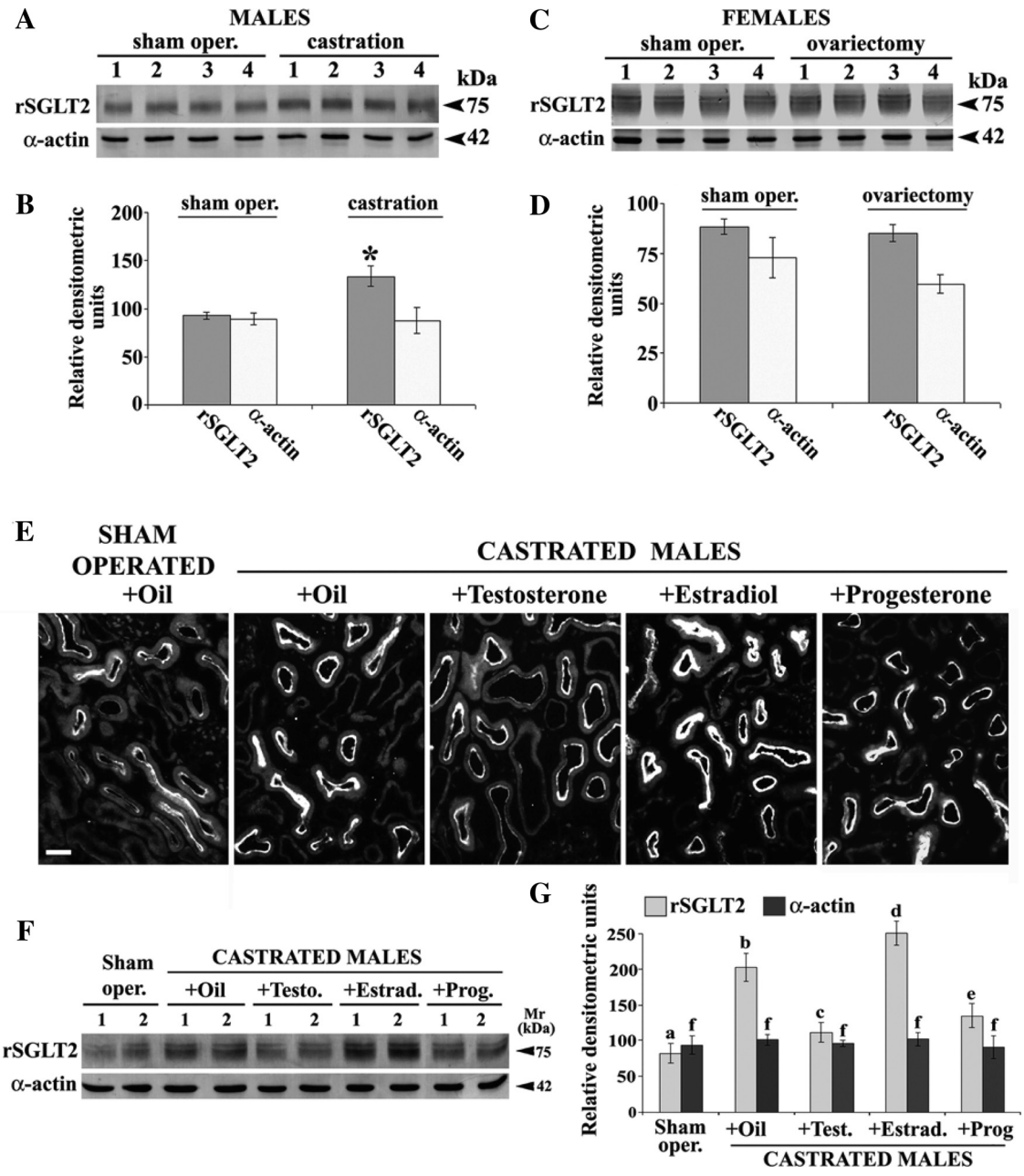


Fig. 4. Effects of gonadectomy in male (M) and female (F) rats (*A–D*) and of sex hormone treatment in castrated M (*E–G*) on renal expression of rSGLT2 protein. *A*: Western blots of rSGLT2 and α-actin in isolated renal cortical BBM from 4 sham-operated and 4 castrated M. *B*: densitometric evaluation of the bands shown in *A*; the rSGLT2-related 75-kDa protein band increased ~50% after castration (vs. sham-operated control rats, $*P < 0.05$), whereas the α-actin band was unaffected by castration. *C*: Western blots of rSGLT2 and α-actin in isolated renal cortical BBM from 4 sham-operated and 4 ovariectomized F. *D*: densitometric quantification of the bands shown in *C*; both the rSGLT2- and α-actin-related bands remained unchanged after ovariectomy. Blots were performed with 40 μg protein/lane. *E*: immunostaining with rSGLT2-Ab in cryosection of the kidney cortex from oil-treated sham-operated adult M and castrated males treated with oil, testosterone, estradiol, or progesterone. In all cases, the staining was abolished after block of the antibody with the immunizing peptide (not shown). Data represent findings in 3 rats from each experimental group. Bar, 20 μm. *F*: representative Western blot of rSGLT2 in TCM from the kidney cortex from sham-operated, castrated, and hormone-treated castrated M. Blots were performed with 60 μg protein/lane. *G*: densitometric quantification of the bands shown in *F* and collected from 2 similar experiments with independent membrane preparations ($N = 4$ in each group). Statistics for the 75-kDa band (ANOVA/ Duncan test): $P < 0.05$: a/b, a/d, a/e, b/c, b/d, and b/e; n.s.: a/c, c/e, and f/f. The density pattern of the 75-kDa protein band in castrated M treated with oil or sex hormones resembled the immunostaining data, i.e., the band was upregulated by castration (2.5-fold), whereas in castrated M it was strongly diminished by testosterone (~50%), increased by estradiol (~20%), and decreased by progesterone (~33%) treatment. The 42-kDa α-actin band was not affected by castration or hormone treatment.

transport whereas the difference between AMG uptake measured in the presence of 20 mM D-galactose and 200 μM phlorizin represented the AMG uptake mediated by rSGLT2 plus NaGLT1. In accordance with our previous data (38), D-galactose-inhibitable AMG transport was significantly higher in BBM vesicles from female versus male kidney cortex, reflecting the higher expression of rSglt1 in female rats. At variance, D-galactose-insensitive, phlorizin-inhibit-

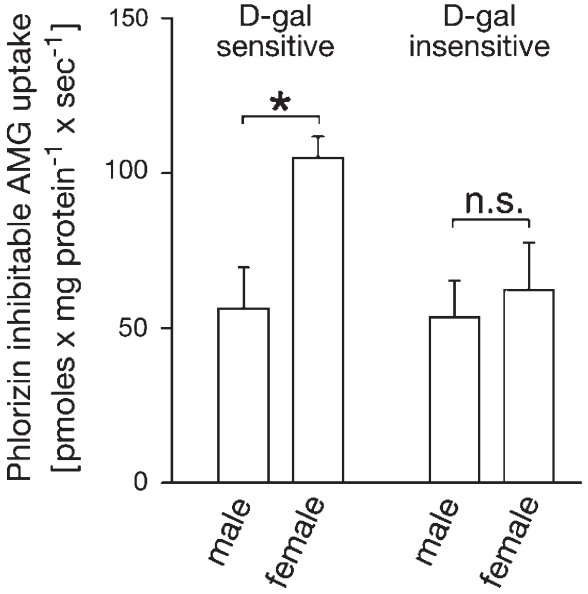


Fig. 5. D-Galactose (D-gal)-sensitive and D-gal-insensitive α-methyl-D-glucopyranoside (AMG) uptake into BBM vesicles isolated from the whole kidneys of male and female rats. The inward $Na^+$ gradient-driven uptake of 0.1 mM [$^{14}$C]AMG was measured by rapid filtration technique in the absence of inhibitors, in the presence of 20 mM D-gal, and in the absence or presence of 0.2 mM phlorizin. AMG uptake in the presence of sodium that can be inhibited by phlorizin represents total $Na^+$-D-glucose cotransport. The D-gal-inhibitable fraction is supposed to represent high-affinity $Na^+$-D-glucose cotransport mediated by rSGLT1 (D-gal sensitive), whereas the D-gal insensitive, phlorizin-inhibitable AMG uptake (D-gal insensitive) represents the low-affinity $Na^+$-D-glucose cotransport, which may be mediated by rSGLT2 and NaGLT1. BBM vesicles from the female cortex exhibited ~85% higher D-gal-inhibitable AMG uptake compared with that in males, whereas the remaining, phlorizin-sensitive, D-gal-insensitive AMG uptake in vesicles from both sexes was similar. Shown are means ± SE of the data collected from studies with 3 different vesicle preparations. *$P < 0.01$.

able AMG uptake was similar in both sexes (Fig. 5). The data suggest that the higher expression of rSGLT2 in BBM of adult females does not manifest in higher activity of low-affinity $Na^+$-D-glucose cotransport.

*SGLT2 in extrarenal organs/tissues in rats.* In an additional set of immunochemical experiments we tested the presence of rSGLT2 protein in various extrarenal organs/tissues (cerebrum, cerebellum, eyes, submaxillary gland, heart, lungs, spleen, pancreas, liver, small intestine, abdominal fat tissue, testes, uterus, skeletal muscle). By immunocytochemistry in cryosections of these organs/tissues from three male and three female rats using high concentrations of rSGLT2-Ab (1:200–1:100) we observed a variable, peptide-blockable staining of some structures; however, at lower concentrations of the antibody (1:5,000–1:1,000), a clear staining was observed only in the kidneys (data not shown). Furthermore, in Western blots of TCM isolated from these extrarenal organs/tissues rSGLT2-Ab labeled various protein bands with higher and/or lower apparent molecular masses than the renal 75-kDa band. All these bands were also blocked by the immunizing peptide (data not shown).

Overall, the preceding immunochemical and mRNA data in rats indicated clear localization and female-dominant expression of the rSGLT2 protein in proximal tubules of the kidney cortex and the presence of cross-reactive proteins in extrarenal organs/tissues. Trying to determine whether the cross-reactive proteins represent splitting products or posttranslationally modified forms of SGLT2, we investigated the expression of SGLT2 protein and its mRNA in various organs of male and female WT mice, using *Sglt2* KO mice as controls for nonspecific reactions.

### *SGLT2 in Mouse Organs*

*SGLT2 in mouse kidneys: immunochemical characterization of rSGLT2-Ab in WT and Sglt2 KO mice.* Expression of mSGLT2 protein in the kidneys and other organs of WT and *Sglt2* KO mice was characterized with the rSGLT2-Ab. As shown by Western blots in Fig. 6*A*, the rSGLT2-Ab strongly stained a single ~75-kDa protein band in BBM from the female rat kidney and a similar, peptide-blockable band in BBM from the WT female mouse kidney. The same band, labeled in TCM from the WT male mouse kidney, was absent in TCM from the *mSglt2* KO male mouse. By immunostaining of the renal cryosections, the rSGLT2-Ab stained the brush border of cortical proximal tubule S1 and S2 segments (S1 > S2) in WT mice (Fig. 6*B*, WT+Ab). The staining was absent with the peptide-blocked antibody (Fig. 6*B*, WT+Ab+P) and in the antibody-treated renal cryosection from the *Sglt2* KO mouse (Fig. 6*B*, KO+Ab). These data confirmed the specificity of rSGLT2-Ab for mSGLT2 protein.

*Zonal and sex differences in renal expression of SGLT2 in adult mice.* A panoramic view of the rSGLT2-related immunostaining in an adult male mouse kidney shows the presence of mSGLT2 protein in the brush border of S1 and S2 proximal tubule segments in the cortex, while the S3 segments in medullary rays and outer stripe as well as the other nephron segments in inner stripe and inner medulla (not shown) remained unstained (Fig. 7*A*). Therefore, the segmental localization of SGLT2 protein in the mouse kidney resembles that in the rat kidney. However, the rSGLT2-Ab-related immunostaining in the kidneys of adult male and female mice revealed the presence of sex differences that are opposite from those in rats; the staining intensity of the brush border in cortical proximal tubules in males was stronger than in females (Fig. 7*B*). The male-dominant protein abundance was confirmed by Western blotting of TCM and BBM isolated from whole kidneys (Fig. 7*C*); the density of the rSGLT2-related 75-kDa protein band was ~110% stronger in the renal membranes from males ($P < 0.05$), whereas the α-actin band density was similar in both sexes (Fig. 7*D*). However, the quantitative RT-PCR data showed that the abundance of *Sglt2* mRNA in the kidneys of adult mice is inversely related to the protein, e.g., it was ~49% higher in females ($P < 0.05$) than in males (Fig. 7*E*).

*Testing SGLT2 protein and its mRNA in various mouse organs of WT and KO mice.* In immunocytochemical studies with rSGLT2-Ab (concentration up to 1:100) in cryosections of various organs/tissues from WT and KO mice, only proximal tubules in the kidney cortex were positive for SGLT2 in WT mice and negative in KO mice; most of the other organs of WT and KO mice did not exhibit any staining, whereas a few organs exhibited a limited, but peptide-blockable staining of some structures in both WT and KO mice (data not shown). Furthermore, Western blots of protein lysates of various organs/tissues from WT male and female mice showed the presence of a ~75-kDa protein band exclusively in the kidneys

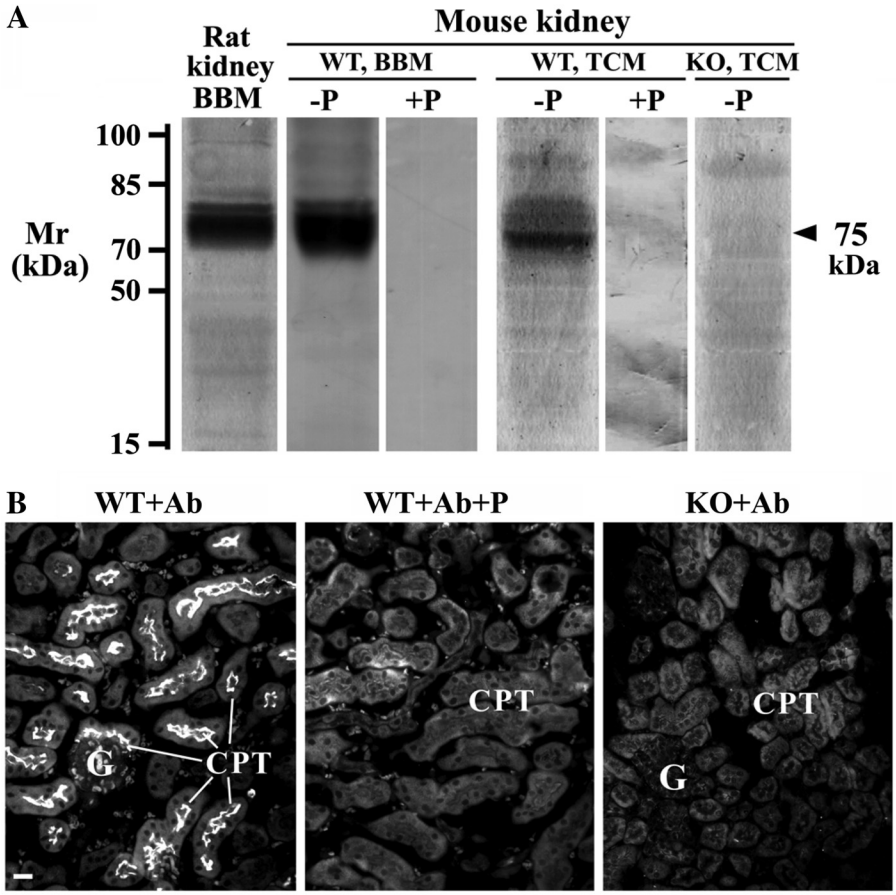


Fig. 6. rSGLT2-Ab-related immunoreactivity in isolated membranes from whole kidneys (*A*) and in cryosections of the kidney cortex (*B*) from wild-type (WT) and *Sglt2* knockout (KO) mice. *A*: Western blots of the rat and mouse renal membranes with rSGLT2-Ab. The antibody labeled the ~75-kDa protein band in the rat renal BBM and in the renal BBM and TCM from WT mice (−P). The band was absent in the membranes from WT mice after application of the peptide-blocked antibody (+P) and in TCM from the *Sglt2* KO mice (KO, TCM; −P). Each lane contained 40 μg (BBM) or 100 μg (TCM) of protein. *B*: immunostaining of SGLT2 in the kidney cortex of WT and KO male mice with rSGLT2-Ab; the antibody stained brush border of the proximal tubules in WT mice (WT+Ab). The staining was absent in WT mice after use of the peptide-blocked antibody (WT+Ab+P) and in KO mice (KO+Ab). G, glomerulus; CPT, cortical proximal tubules. Bar, 20 μm.

(Fig. 8). We therefore conclude that in mice the kidney is the only organ with a significant expression of SGLT2 protein.

Absence of SGLT2 in the mouse extrarenal organs was confirmed at the mRNA level (Fig. 9). Whereas the expression of housekeeping gene *rpl19* mRNA was similar in various organs/tissues from WT male and female mice (Fig. 9*A*), *Sglt2* mRNA was expressed only in the kidney; in other organs in WT animals, as well as in the kidneys of KO mice, *mSglt2* mRNA was not detected (Fig. 9*B*).

## DISCUSSION

In this study we describe a novel antibody against rSGLT2 that allows a detailed immunochemical localization of this transporter in the rat kidneys. In comparison, previously described antibodies against SGLT2 from different species did not reveal distinct immunochemical characterization of this protein (2, 7, 19, 35, 50). Our new antibody labeled a broad ~75-kDa protein band in Western blots of BBM or TCM isolated from the rat renal cortex and did not cross-react with rSGLT1 and rSGLT3, as indicated by the lack of reactivity with small intestine, where these transporters are expressed (5, 16, 38). Because of cross-reactivity of the rSGLT2-Ab with mouse SGLT2, a similar broad protein band of ~75 kDa was also labeled in renal TCM and BBM of mice (Fig. 6 and Ref. 48). Since in the *Sglt2* KO mice no labeling of a broad protein band of ~75 kDa was observed (Fig. 6 and Ref. 48) we conclude that this protein band, labeled with the rSGLT2-Ab in the rat and mouse renal membranes, represents the SGLT2 protein. In some Western blots, the broad ~75-kDa band was dissolved into two or three individual bands. So far we were not able to distinguish whether this heterogeneity of rSGLT2 protein is due to different degrees of glycosylation, phosphorylation, or proteolytic cleavage.

Consistent with the previously described location of *rSglt2* mRNA by in situ hybridization (54), in rats we confirmed localization of the rSGLT2 protein in the brush border of renal proximal tubule S1 and S2 segments (S1 > S2) and its absence in the S3 segment. The renal location of rSGLT2 matches the assumption that a high-capacity SGLT2 represents the D-galactose-insensitive low-affinity $Na^+$-D-glucose cotransport system localized in the early segments of renal proximal tubules, as has been indicated by different methods in previous studies in rat, mouse, and rabbit kidneys (4, 21, 45, 48, 54). This is probably also true for humans, because homozygous defect mutations of SGLT2 lead to renal glucosuria with almost complete absence of D-glucose reabsorption in proximal tubules (39, 40). Previous studies in SGLT2-deficient mice demonstrated that SGLT2 protein is expressed and mediates all glucose reabsorption in the early proximal tubule and most of the glucose reabsorption by the kidney overall (48). In mice, D-glucose remaining in the late distal tubule is mainly reabsorbed by the high-affinity transporter SGLT1 (16); however, in rats the recently cloned low-affinity $Na^+$-D-glucose cotransporter NaGLT1 may contribute significantly to the reabsorption of D-glucose in proximal tubules (22). Like

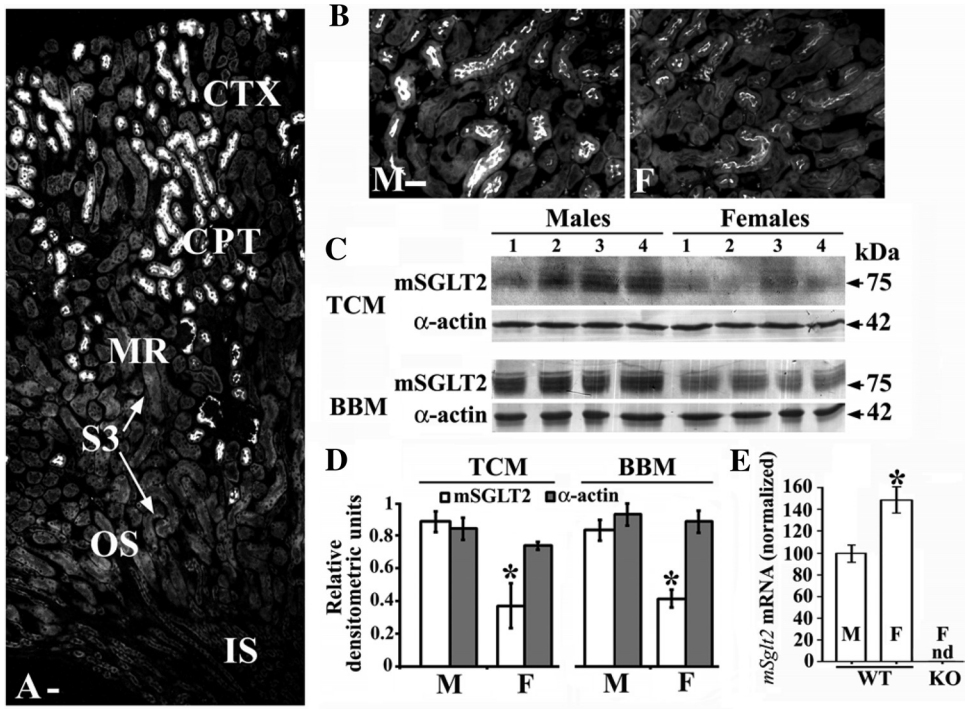


Fig. 7. Zonal distribution (*A*) and sex-dependent expression of SGLT2 in kidneys of adult mice (*B–E*). *A*: zonal distribution; in the kidney of male mice, rSGLT2-Ab stained the brush border of cortical proximal tubules (S1/S2 segments; CPT), whereas the S3 segments in medullary rays (MR) and outer stripe (OS) remained unstained. Data represent findings in 3 male mice. CTX, cortex; IS, inner stripe. *B*: immunostaining of SGLT2 in cortical proximal tubules in an adult male (M) and an adult female (F) rat. The staining intensity of the proximal tubule brush border in the M was stronger than in the F. Data represent findings in 3 mice of each sex. Bars in *A* and *B*, 20 μm. *C*: abundance of mSGLT2 protein and actin in TCM and BBM isolated from the whole kidneys of 4 adult M and F. Each lane contained 80 μg (TCM) or 50 μg (BBM) protein. *D*: densitometric evaluation of the bands shown in *C*. TCM: data were collected from 2 independent studies with 4 membrane preparations in each experiment ($N = 8$ in each bar). BBM: each membrane sample was prepared from the pool of kidneys from 3 animals of the respective sex ($N = 4$ in each bar). The mSGLT2-related 75-kDa protein band in M was ~2.4-fold (TCM) or ~2.1-fold (BBM) stronger compared with F ($^*P < 0.05$), whereas the actin-related 42-kDa protein band showed no sex differences. *E*: expression of *rSglt2* mRNA in kidneys of WT and KO mice as estimated by real-time RT-PCR ($N = 6$ for each sex). In WT mice the expression in F was ~49% stronger than in M ($^*P < 0.05$), whereas in *Sglt2* KO F mRNA was not detected (nd).

rSGLT2, NaGLT1 is also located in the BBM of renal proximal tubules and does not accept D-galactose as substrate.

The expression of rSGLT2 in rat renal proximal tubules is influenced by sex hormones as has been demonstrated for rSGLT1 (38), organic anion transporters rOAT1, rOAT2, rOAT3, and rOAT5 (11, 29, 30), and organic cation transporter rOCT2 (46). Similar to rSGLT1, female rats showed a higher expression of rSGLT2 in proximal tubules compared with males. However, whereas rSGLT1 was upregulated at the level of transcription, the higher expression of rSGLT2 in females versus males is apparently due to posttranscriptional regulation. The observed lack of correlation between the higher amount of rSGLT2 protein in BBM vesicles of female versus male rats and $Na^+$-dependent AMG uptake in the presence of D-galactose (data in Fig. 5) may have different reasons. There may be a compensatory upregulation of rNaGLT1-mediated glucose transport in males versus females. Another possibility is that an additional sex-dependent regulation of transporter turnover (activity of individual rSGLT2 molecules) compensates for a larger amount of rSGLT2 protein in females versus males. This type of regulation may be mediated by different posttranscriptional modifications, different interactions with other proteins, and/or different lipid microenvironments (1). However, in our transport studies we also cannot exclude a possible contribution of SGLT5 (*SLC5A9*), whose mRNA was detected in bovine (58), rabbit (53), and pig (3) kidneys, but the renal localization and functional characterization of SGLT5 protein in these animals, as well as both mRNA and protein expression in rodent kidneys, have not been reported.

Treating gonadectomized rats with sex hormones, we observed that rSGLT2 was strongly downregulated by androgens, as also described for rSGLT1 (38). However, whereas the renal expression of rSGLT1 was not altered by estrogens (5, 38), the expression of rSGLT2 was also downregulated by progesterone and weakly upregulated by estradiol (data in Fig. 4). A downregulating effect of progesterone may play a role in pregnancy, which is characterized by elevated levels of placenta-derived progesterone and, often, glucosuria (17). Since ovariectomy did not significantly affect expression of SGLT2, the weak upregulation observed after estradiol treatment may be due to the high pharmacological dose applied. Our data indicate that sex hormone-dependent regulation of $Na^+$-D-glucose cotransporters in rat kidney is complex and develops with sexual maturation. Regulation of two or possibly three individual $Na^+$-D-glucose cotransporters and transcriptional and posttranscriptional mechanisms may be involved.

Our immunochemical experiments did not reveal the presence of rSGLT2 protein in extrarenal organs/tissues in rats. Immunizing peptide-blockable staining of some structures in several extrarenal organs with a high concentration of the rSGLT2-Ab (not shown in results) probably represented cross-reactions with similar epitopes on tertiary structures of unre-

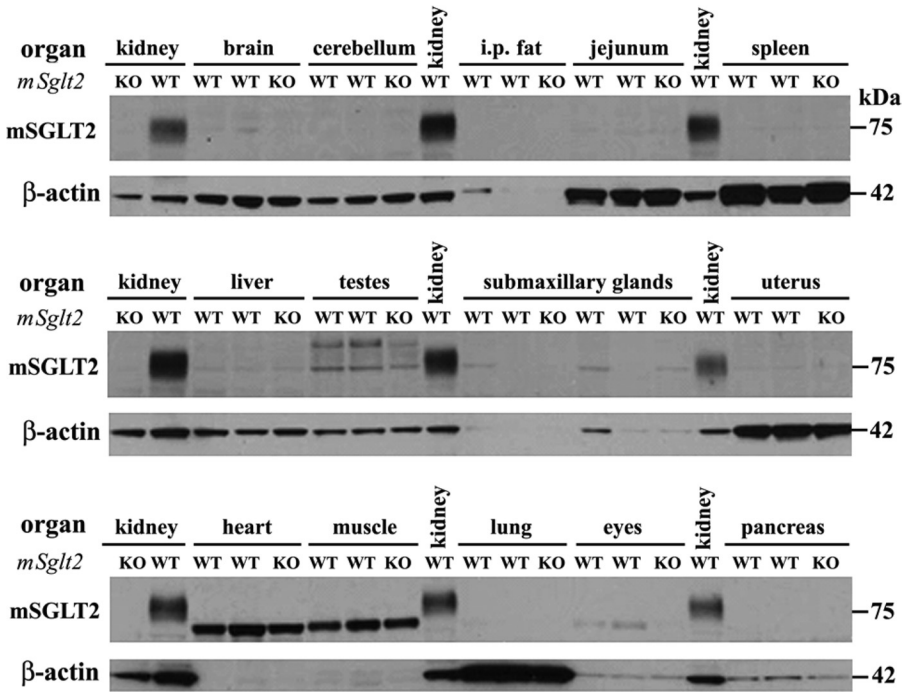


Fig. 8. Absence of SGLT2 protein expression in extrarenal organs of the mouse. Western blot analysis was performed in protein lysate of various organs from 2 male and 2 female WT mice. Kidneys of WT mice served as positive control, and kidneys of KO (*Sglt2*$^{-/-}$) mice were used as negative control. In the kidneys of WT mice the rSGLT2-Ab recognized a protein band of the predicted size of SGLT2 (~75 kDa), whereas in other organs the antibody recognized additional unspecific bands. In none of the studied extrarenal WT organs was a band consistently detected that corresponded in size to the SGLT2-related band detected in WT kidney. Each lane was loaded with 10 μg of whole organ lysate. β-Actin was used to confirm equal loading, although its expression varies between organs. i.p., Intraperitoneal.

lated proteins, and thus indicates the possibility of misinterpretation of immunocytochemical staining. Extrarenal expression of *Sglt2* mRNA in several species has been previously proposed in kidney, liver, lung, spleen, eye, and mammary gland of several species (12, 25, 41, 51, 54, 57); however, the cellular location of SGLT2 protein has not been determined. A more recent study with quantitative PCR analysis indicated a highly kidney-specific expression of *Sglt2* mRNA in humans (13). Recently, expression of rSGLT1 in rat brain neurons has been attributed to distinct areas such as thalamus and hippocampus, and the functional significance of phlorizin-inhibitable $Na^+$-D-glucose cotransporters for D-glucose uptake into rat brain has been demonstrated with the use of a glucose analog that can pass the blood-brain barrier (55). In these experiments the involvement of rSGLT2 was proposed based on the observation that only part of the phlorizin-inhibitable glucose uptake could be inhibited by the SGLT1-blocking agent D-galactose. In human hearts, $Na^+$-D-glucose cotransport contributes significantly to D-glucose uptake in physiological conditions and is supposed to gain a pivotal role during heart failure and after ischemia when the main energy supply of the heart shifts from fatty acids to glucose (28). Human hearts contain a large amount of *Sglt1* mRNA located in the myocytes but no significant amount of *Sglt2* mRNA (13, 28, 59).

Since our immunochemical experiments in rats did not yield unequivocal results regarding the presence of rSGLT2 protein

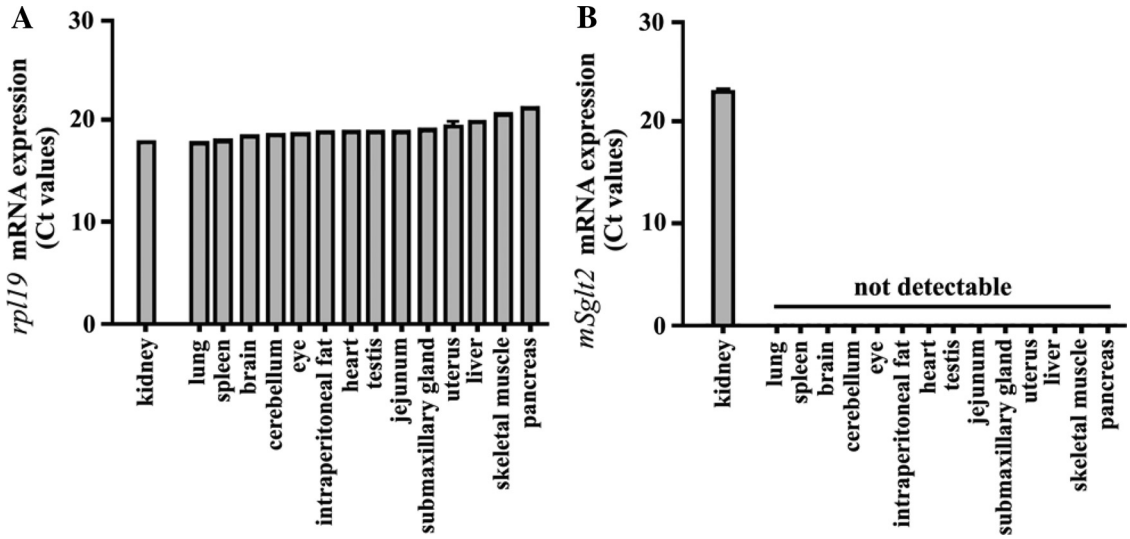


Fig. 9. Absence of *Sglt2* mRNA expression in extrarenal organs of the mouse. Cycle thresholds ($C_t$) are indicated, and 50 cycles were performed. *A*: expression of housekeeping gene *rpl19* mRNA. *B*: expression of *Sglt2* mRNA. Kidney tissue served as a positive control for *Sglt2* mRNA expression. Kidneys of *Sglt2* KO mice were used as negative controls (not shown). Data are collected from determination in 6 (3 male and 3 female) WT mice. Error bars are too small to be seen.

in extrarenal organs/tissues, we have tested the expression of SGLT2 at the protein and mRNA levels in male and female WT and *Sglt2* KO mice. With three independent methods, e.g., immunocytochemistry in tissue cryosections (not shown), Western blotting of tissue lysates (Fig. 8), and real-time RT-PCR (Fig. 9), we found that the expression of SGLT2 protein and *Sglt2* mRNA are kidney-specific in mice; no significant specific signal was observed in the tested extrarenal organs/tissues of WT mice.

Whereas the localization experiments in the kidneys of WT mice showed distribution of the protein in S1 and S2 proximal tubule segments (S3 was negative), which is similar to that in rats, its abundance in the renal membranes in mice was strongly male dominant, which is opposite from that in rats (female dominant). These sex differences in the transporter expression in mice may be related to the data in our previous study in BBM vesicles from the kidney cortex of adult male and female BALB/c mice, where the $Na^+$ gradient-driven intravesicular uptake of D-glucose was ~2.5-fold higher in males then in females and after testosterone treatment of females it rose to the levels in males (32). These data thus indicate that androgens have major, but species-specific, effect in regulating the renal expression of SGLT2 protein in mice (stimulation) and rats (inhibition).

Our previous study in rats (38) showed that both expression of rSGLT1 protein in the proximal tubule brush border and phlorizin/galactose-sensitive glucose transport in isolated BBM are female dominant. The expression of rSGLT2 protein in rat proximal tubules was also female dominant but not accompanied by higher SGLT2-specific uptake in brush-border vesicles. In addition to these species differences in expression of SGLT1 and SGLT2 proteins, different mechanisms of sex-dependent regulations were observed: In rat kidneys a higher concentration of *Sglt1* mRNA was observed in females versus males (38), while the concentrations of *Sglt2* mRNA were identical in males and females (Fig. 3). In contrast, the expression of renal *Sglt2* mRNA in mice is strongly female dominant and opposite from the male-dominant SGLT2 protein expression (this report, Fig. 7). These data point to several mechanisms regulating the expression of renal SGLTs in rodents that may occur at the transcriptional and/or posttranscriptional levels.

In conclusion, we have provided evidence that in rats SGLT2 is located in the BBM of S1 and S2 segments (S1 > S2) of renal proximal tubules with female-dominant expression, posttranscriptionally upregulated by sex hormones after puberty. In mice, the SGLT2 protein is also localized in the BBM of renal cortical proximal tubule S1/S2 segments, but with male-dominant expression, whereas the expression of its mRNA is opposite, i.e., female dominant. Using the *Sglt2* KO mice model as a negative control, our studies indicate a kidney-specific expression of both SGLT2 protein and *Sglt2* mRNA in mice. The existence of sex and species differences in the expression of renal SGLT2 should be taken into consideration in pharmacological testing of specific inhibitors of glucose transporters in humans.

## ACKNOWLEDGMENTS

The authors thank Eva Heršak for technical assistance and Dr. Sanja Milković-Kraus for constructive discussions.

We thank the Wellcome Trust Sanger Institute Mouse Genetics Project and Lexicon Pharmaceuticals for providing *Sglt2* WT and KO mice. Associated primary phenotypic information can be found at **www.sanger.ac.uk/mouseportal**.

## GRANTS

This work was supported by Grants 022-0222148-2146 (Ministry for Science, Education and Sports, Republic of Croatia; to I. Sabolić) and SFB 487/C1 (Deutsche Forschungsgemeinschaft; to H. Koepsell), National Institute of Health Grants R01 DK-56248, R01 HL-94728, and P30 DK-079337 and the Department of Veterans Affairs (all to V. Vallon), and TH1430/3-1 (Deutsche Forschungsgemeinschaft) and the Focus Program Translational Neurosciences (FTN) of the Johannes Gutenberg-University, Mainz, Germany (both to S. C. Thal).

## DISCLOSURES

V. Vallon's research was partially supported by grants provided by Bristol-Myers Squibb and Astra Zeneca.

## AUTHOR CONTRIBUTIONS

Author contributions: I.S., S.C.T., V.V., and H. Koepsell conception and design of research; I.S., I.V., D.B.E., M.G., M.R., D.B., H.B., A.S., S.C.T., C.S., H. Kipp, V.V., and H. Koepsell analyzed data; I.S., D.B., M.L., H.B., S.C.T., C.S., H. Kipp, V.V., and H. Koepsell interpreted results of experiments; I.S., I.V., and D.B.E. drafted manuscript; I.S., S.C.T., V.V., and H. Koepsell edited and revised manuscript; I.S., S.C.T., V.V., and H. Koepsell approved final version of manuscript; I.V., D.B.E., M.G., M.R., D.B., M.L., H.B., A.S., C.S., and H. Kipp performed experiments; I.V., D.B.E., M.G., M.R., M.L., A.S., and C.S. prepared figures.

## REFERENCES

1. **Albertoni Borghese MF, Majowicz MP, Ortiz MC, Passalacqua MR, Sterin Speziale NB, Vidal NA.** Expression and activity of SGLT2 in diabetes induced by streptozotocin: relationship with the lipid environment. *Nephron Physiol* 112: P45–P52, 2009.
2. **Aljure O, Diez-Sampedro A.** Functional characterization of mouse sodium/glucose transporter type 3b. *Am J Physiol Cell Physiol* 299: C58–C65, 2010.
3. **Aschenbach JR, Steglich K, Gabel G, Honscha KU.** Expression of mRNA for glucose transport proteins in jejunum, liver, kidney and skeletal muscle of pigs. *J Physiol Biochem* 65: 251–266, 2009.
4. **Bakris GL, Fonseca VA, Sharma K, Wright EM.** Renal sodium-glucose transport: role in diabetes mellitus and potential clinical implications. *Kidney Int* 75: 1272–1277, 2009.
5. **Balen D, Ljubojevic M, Breljak D, Brzica H, Zlender V, Koepsell H, Sabolic I.** Revised immunolocalization of the $Na^+$-D-glucose cotransporter SGLT1 in rat organs with an improved antibody. *Am J Physiol Cell Physiol* 295: C475–C489, 2008.
6. **Barfuss DW, Schafer JA.** Differences in active and passive glucose transport along the proximal nephron. *Am J Physiol Renal Fluid Electrolyte Physiol* 240: F322–F332, 1981.
7. **Bautista R, Manning R, Martinez F, Avila-Casado MC, Soto V, Medina A, Escalante B.** Angiotensin II-dependent increased expression of $Na^+$-glucose cotransporter in hypertension. *Am J Physiol Renal Physiol* 286: F127–F133, 2004.
8. **Bell GI, Burant CF, Takeda J, Gould GW.** Structure and function of mammalian facilitative sugar transporters. *J Biol Chem* 268: 19161–19164, 1993.
9. **Biber J, Stieger B, Haase W, Murer H.** A high yield preparation for rat kidney brush border membranes: different behaviour of lysosomal markers. *Biochim Biophys Acta* 647: 169–176, 1981.
10. **Bradford MM.** A rapid and sensitive method for the quantitation of microgram quantities of protein utilizing the principle of protein-dye binding. *Anal Biochem* 72: 248–254, 1976.
11. **Breljak D, Ljubojevic M, Balen D, Zlender V, Brzica H, Micek V, Kusan M, Anzai N, Sabolic I.** Renal expression of organic anion transporter Oat5 in rats and mice exhibits the female-dominant sex differences. *Histol Histopathol* 25: 1385–1402, 2010.
12. **Chan CY, Guggenheim JA, To CH.** Is active glucose transport present in bovine ciliary body epithelium? *Am J Physiol Cell Physiol* 292: C1087–C1093, 2007.

13. **Chen J, Williams S, Ho S, Loraine H, Hagan D, Whaley JM, Feder JN.** Quantitative PCR tissue expression profiling of the human SGLT2 gene and related family members. *Diabetes Ther* 1: 57–92, 2010.
14. **Diez-Sampedro A, Hirayama BA, Osswald C, Gorboulev V, Baumgarten K, Volk C, Wright EM, Koepsell H.** A glucose sensor hiding in a family of transporters. *Proc Natl Acad Sci USA* 100: 11753–11758, 2003.
15. **Elfeber K, Stümpel F, Gorboulev V, Mattig S, Deussen A, Kaissling B, Koepsell H.** $Na^+$-D-glucose cotransporter in muscle capillaries increases glucose permeability. *Biochem Biophys Res Commun* 314: 301–305, 2004.
16. **Gorboulev V, Schürmann A, Vallon V, Kipp H, Jaschke A, Klessen D, Friedrich A, Scherneck S, Rieg T, Cunard R, Veyhl-Wichmann M, Srinivasan A, Balen D, Breljak D, Rexhepaj R, Parker HE, Gribble FM, Reimann F, Lang F, Wiese S, Sabolic I, Sendtner M, Koepsell H.** $Na^+$-D-glucose cotransporter SGLT1 is pivotal for intestinal glucose absorption and glucose-dependent incretin secretion. *Diabetes* 61: 187–196, 2012.
17. **Gribble RK, Meier PR, Berg RL.** The value of urine screening for glucose at each prenatal visit. *Obstet Gynecol* 86: 405–410, 1995.
18. **Han HJ, Lee YJ, Park SH, Lee JH, Taub M.** High glucose-induced oxidative stress inhibits $Na^+$/glucose cotransporter activity in renal proximal tubule cells. *Am J Physiol Renal Physiol* 288: F988–F996, 2005.
19. **Han HJ, Park SH, Lee YJ.** Signaling cascade of ANG II-induced inhibition of α-MG uptake in renal proximal tubule cells. *Am J Physiol Renal Physiol* 286: F634–F642, 2004.
20. **Handlon AL.** Sodium glucose co-transporter 2 (SGLT2) inhibitors as potential antidiabetic agents. *Exp Opin Therapeut Patents* 15: 1531–1540, 2005.
21. **Hediger MA, Rhoads DB.** Molecular physiology of sodium-glucose cotransporters. *Physiol Rev* 74: 993–1026, 1994.
22. **Horiba N, Masuda S, Takeuchi A, Takeuchi D, Okuda M, Inui KI.** Cloning and characterization of a novel $Na^+$-dependent glucose transporter (NaGLT1) in rat kidney. *J Biol Chem* 278: 14669–14676, 2003.
23. **Idris I, Donnelly R.** Sodium-glucose co-transporter-2 inhibitors: an emerging new class of oral antidiabetic drug. *Diabetes Obes Metab* 11: 79–88, 2009.
24. **Jabbour SA, Goldstein BJ.** Sodium glucose co-transporter 2 inhibitors: blocking renal tubular reabsorption of glucose to improve glycaemic control in patients with diabetes. *Int J Clin Pract* 62: 1279–1284, 2008.
25. **Kanai Y, Lee WS, You G, Brown D, Hediger MA.** The human kidney low affinity $Na^+$/glucose cotransporter SGLT2; delineation of the major renal reabsorptive mechanism for D-glucose. *J Clin Invest* 93: 397–404, 1994.
26. **Kong CT, Yet SF, Lever JE.** Cloning and expression of a mammalian $Na^+$/amino acid cotransporter with sequence similarity to $Na^+$/glucose cotransporters. *J Biol Chem* 268: 1509–1512, 1993.
27. **Kroiss M, Leyerer M, Gorboulev V, Kühlkamp T, Kipp H, Koepsell H.** Transporter regulator RS1 (*RSC1A1*) coats the *trans*-Golgi network and migrates into the nucleus. *Am J Physiol Renal Physiol* 291: F1201–F1212, 2006.
28. **von Lewinski D, Gasser R, Rainer PP, Huber MS, Wilhelm B, Roessl U, Haas T, Wasler A, Grimm M, Bisping E, Pieske B.** Functional effects of glucose transporters in human ventricular myocardium. *Eur J Heart Fail* 12:106–113, 2010. o.
29. **Ljubojevic M, Balen D, Breljak D, Kusan M, Anzai N, Bahn A, Burckhardt G, Sabolic I.** Renal expression of organic anion transporter OAT2 in rats and mice is regulated by sex hormones. *Am J Physiol Renal Physiol* 292: F361–F372, 2007.
30. **Ljubojevic M, Herak-Kramberger CM, Hagos Y, Bahn A, Endou H, Burckhardt G, Sabolic I.** Rat renal cortical OAT1 and OAT3 exhibit gender differences determined by both androgen stimulation and estrogen inhibition. *Am J Physiol Renal Physiol* 287: F124–F138, 2004.
31. **Mackenzie B, Panayotova-Heiermann M, Loo DDF, Lever JE, Wright EM.** SAAT1 is a low affinity $Na^+$/glucose cotransporter and not an amino acid transporter. *J Biol Chem* 269: 22488–22491, 1994.
32. **Mackovic M, Zimolo Z, Burckhardt G, Sabolic I.** Isolation of renal brush-border membrane vesicles by a low speed centrifugation; effect of sex hormones on $Na^+$-$H^+$ exchange in rat and mouse kidney. *Biochim Biophys Acta* 862: 141–152, 1986.
33. **Martin MG, Turk E, Lostao MP, Kerner C, Wright EM.** Defects in $Na^+$/glucose cotransporter (SGLT1) trafficking and function cause glucose-galactose malabsorption. *Nat Genet* 12: 216–220, 1996.
34. **Panayotova-Heiermann M, Loo DDF, Wright EM.** Kinetics of steady-state currents and charge movements associated with the rat $Na^+$/glucose cotransporter. *J Biol Chem* 270: 27099–27105, 1995.
35. **Rahmoune H, Thompson PW, Ward JM, Smith CD, Hong G, Brown J.** Glucose transporters in human renal proximal tubular cells isolated from the urine of patients with non-insulin-dependent diabetes. *Diabetes* 54: 3427–3434, 2005.
36. **Sabolic I, Asif AR, Budach WE, Wanke C, Bahn A, Burckhardt G.** Gender differences in kidney function. *Pflügers Arch* 455: 397–429, 2007.
37. **Sabolic I, Culic O, Lin SH, Brown D.** Localization of ecto-ATPase in rat kidney and isolated renal cortical membrane vesicles. *Am J Physiol Renal Fluid Electrolyte Physiol* 262: F217–F228, 1992.
38. **Sabolic I, Skarica M, Gorboulev V, Ljubojevic M, Balen D, Herak-Kramberger CM, Koepsell H.** Rat renal glucose transporter SGLT1 exhibits zonal distribution and androgen-dependent gender differences. *Am J Physiol Renal Physiol* 290: F913–F926, 2006.
39. **Santer R, Kinner M, Lassen CL, Schneppenheim R, Eggert P, Bald M, Brodehl J, Daschner M, Ehrich JHH, Kemper M, Li Volti S, Neuhaus T, Skovby F, Swift PGF, Schaub J, Klaerke D.** Molecular analysis of the *SGLT2* gene in patients with renal glucosuria. *J Am Soc Nephrol* 14: 2873–2882, 2003.
40. **Scholl-Bürgi S, Santer R, Ehrich JHH.** Long-term outcome of renal glucosuria type 0: the original patient and his natural history. *Nephrol Dial Transplant* 19: 2394–2396, 2004.
41. **Tabatabai NM, Blumenthal SS, Lewand DL, Petering DH.** Mouse kidney expresses mRNA of four highly related sodium-glucose cotransporters: regulation by cadmium. *Kidney Int* 64: 1320–1330, 2003.
42. **Tabatabai NM, Sharma M, Blumenthal SS, Petering DH.** Enhanced expressions of sodium-glucose cotransporters in the kidneys of diabetic Zucker rats. *Diabetes Res Clin Pract* 83: e27–e30, 2009.
43. **Takahashi K, Masuda S, Nakamura N, Saito H, Futami T, Doi T, Inui KI.** Upregulation of $H^+$-peptide cotransporter PEPT2 in rat remnant kidney. *Am J Physiol Renal Physiol* 281: F1109–F1116, 2001.
44. **Turk E, Zabel B, Mundlos S, Dyer J, Wright EM.** Glucose/galactose malabsorption caused by a defect in the $Na^+$/glucose cotransporter. *Nature* 350: 354–356, 1991.
45. **Turner RJ, Moran A.** Heterogeneity of sodium-dependent D-glucose transport sites along the proximal tubule: evidence from vesicle studies. *Am J Physiol Renal Fluid Electrolyte Physiol* 242: F406–F414, 1982.
46. **Urakami Y, Nakamura N, Takahashi K, Okuda M, Saito H, Hashimoto Y, Inui KI.** Gender differences in expression of organic cation transporter OCT2 in rat kidney. *FEBS Lett* 461: 339–342, 1999.
47. **Vallon V.** The proximal tubule in the pathophysiology of the diabetic kidney. *Am J Physiol Regul Integr Comp Physiol* 300: R1009–R1022, 2011.
48. **Vallon V, Platt KA, Cunard R, Schroth J, Whaley J, Thomson SC, Koepsell H, Rieg T.** SGLT2 mediates glucose reabsorption in the early proximal tubule. *J Am Soc Nephrol* 21: 104–112, 2011.
49. **Vernaleken A, Veyhl M, Gorboulev V, Kottra G, Palm D, Burckhardt BC, Burckhardt G, Pipkorn R, Beier N, van Amsterdam C, Koepsell H.** Tripeptides of RS1 (*RSC1A1*) inhibit a monosaccharide-dependent exocytotic pathway of $Na^+$-D-glucose cotransporter SGLT1 with high affinity. *J Biol Chem* 282: 28501–28513, 2007.
50. **Vestri S, Okamoto MM, de Freitas HS, Aparecida dos Santos R, Nunes MT, Morimatsu M, Heimann JC, Machado UF.** Changes in sodium or glucose filtration rate modulate expression of glucose transporters in renal proximal tubular cells of rat. *J Membr Biol* 182: 105–112, 2001.
51. **Wells RG, Pajor AM, Kanai Y, Turk E, Wright EM, Hediger MA.** Cloning of a human kidney cDNA with similarity to the sodium-glucose cotransporter. *Am J Physiol Renal Fluid Electrolyte Physiol* 263: F459–F465, 1992.
52. **Wright EM, Martin MG, Turk E.** Intestinal absorption in health and disease-sugars. *Best Pract Res Clin Gastroenterol* 17: 943–956, 2003.
53. **Wright EM, Turk E.** The sodium/glucose cotransport family SLC5. *Pflügers Arch* 447: 510–518, 2004.
54. **You G, Lee WS, Barros EJG, Kanai Y, Huo TL, Khawaja S, Wells RG, Nigam SK, Hediger MA.** Molecular characteristics of $Na^+$-coupled glucose transporters in adult and embryonic rat kidney. *J Biol Chem* 270: 29365–29371, 1995.
55. **Yu AS, Hirayama BA, Timbol G, Liu J, Basarah E, Kepe V, Satyamurthy N, Huang SC, Wright EM, Barrio JR.** Functional expression of SGLTs in rat brain. *Am J Physiol Cell Physiol* 299: C1277–C1284, 2010.

56. **Zhao FQ, Keating AF.** Expression and regulation of glucose transporters in the bovine mammary gland. *J Dairy Sci* 90, Suppl E: E76–E86, 2007.
57. **Zhao FQ, McFadden TB, Wall EH, Dong B, Zheng YC.** Cloning and expression of bovine sodium/glucose cotransporter SGLT2. *J Dairy Sci* 88: 2738–2748, 2005.
58. **Zhao FQ, Zheng YC, Wall EH, McFadden TB.** Cloning and expression of bovine sodium/glucose cotransporters. *J Dairy Sci* 88: 182–194, 2005.
59. **Zhou L, Cryan EV, D'Andrea MR, Belkowski S, Conway BR, Demarest KT.** Human cardiomyocytes express high level of $Na^+$/glucose cotransporter 1 (SGLT1). *J Cell Biochem* 90: 339–346, 2003.